Bound Photon Orbits and Critical Parameters in Kerr de Sitter space times.

Eunice Omwoyo,

Verao Quantico 2023

Agenda

1. Motivation
2. Kerr de Sitter
3. Analytical Ray Tracing
4. Conclusion

General Information

- The Event Horizon Telescope has shown the images at the centre of M87* and Sagittarius A (Sgr A).

Figura 1: M87.

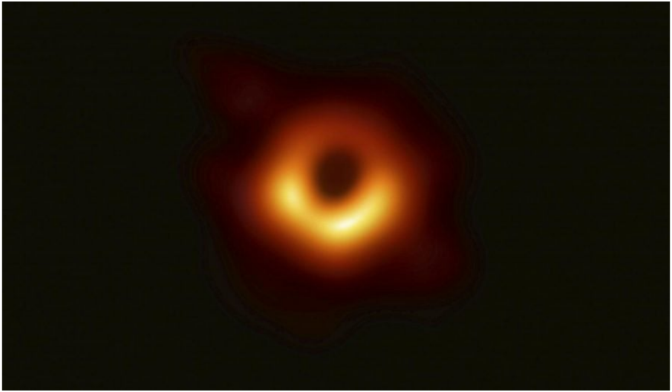

Figura 2: Sagittarius A.

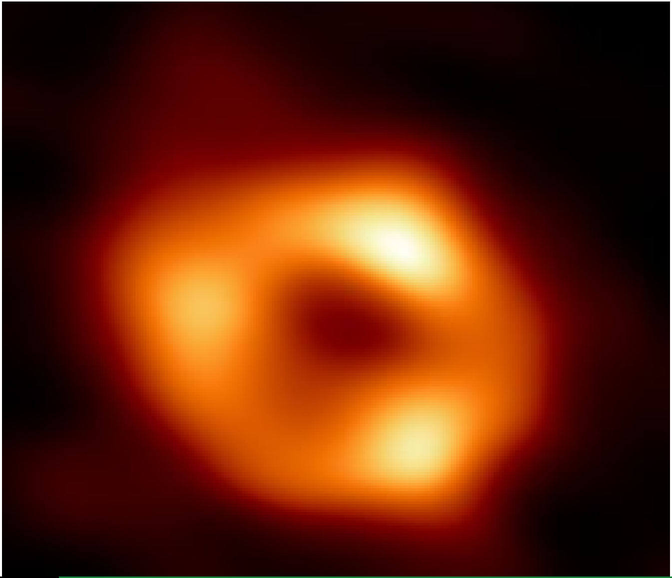

What does the future hold?

Sharper and sharper images will hopefully be captured as time passes. The crucial question is, what should be seen when sharp images are captured (high resolution)?

Figura 3: General Relativistic Magneto hydrodynamics (GRMHD) simulation of a black hole shadow.

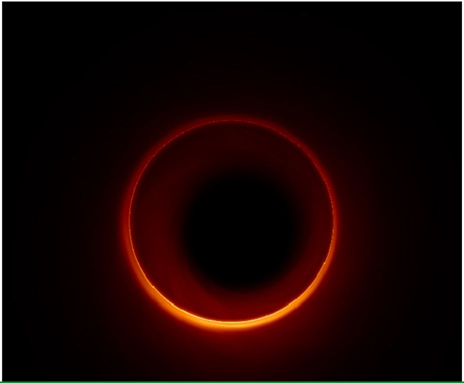

Can this image teach us anything about GR?

The nature of GR in regimes of strong gravity predicts a circular shape. Will clearer images show a circular shaped ring?

What is the origin of the photon ring ?

What other things can this image help in attaining?

- Putting strong constraints on the black hole parameters.
- Cosmological studies: In an expanding universe, the size of the shadow can aid in constraining the Hubble constant.

Structure of the Photon Ring

- The photon ring is composed of self similar subrings indexed by the number of photon orbits (n=0,1,2...∞) around the black hole. n=∞: Bound photon orbits, n=$1, 2, 3$..: Nearly bound orbits.
- These subrings are entirely governed by three critical parameters.

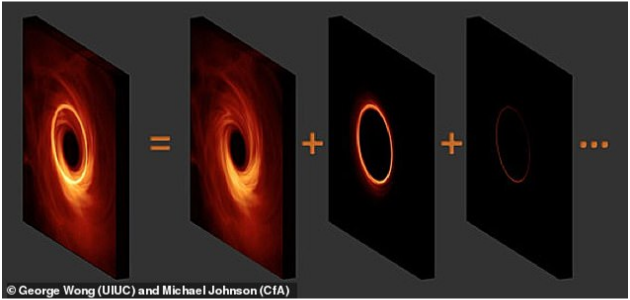

- The photon ring is not only visible in the image but also in the Fourier Transform of the image.
- Thus the sub-rings produce signatures on Very Long Baseline Interferometers (VLBI) that could be detected using space-based interferometers.

What can be learnt from the photon ring

- Since the photon ring is matter independent, measuring it can then provide a test of general relativity and gravity in the strong field regime.

How can we understand the photon ring

- To understand the photon ring, knowledge of bound photon orbits is crucial.
- In this work, we will study the bound photon orbits in Kerr de Sitter (KdS) space time and Kerr de Sitter Revisited space time.
- In so doing we will derive the three critical parameters (δ, γ and ζ) that govern the sub-rings in KdS space time.
- Moreover, we will obtain solutions that will yield nearly bound photon orbits.

KdS

The null geodesic equations in KdS space time are given as,

$$\frac{\Sigma}{E}p^r = \pm_r\sqrt{R(r)}, \frac{\Sigma}{E}p^\theta = \pm_\theta\sqrt{\Theta(\theta)}, \tag{1}$$

$$\frac{\Sigma}{E}p^\phi = \frac{aL^2}{\Delta_r}(a(a-\lambda)+r^2) - \frac{L^2}{\Delta_\theta \sin^2\theta}(a\sin^2\theta - \lambda), \tag{2}$$

$$\frac{\Sigma}{E}p^t = \frac{L^2}{\Delta_r}((r^2+a^2)^2 - a\lambda(a^2+r^2)) - \frac{aL^2}{\Delta_\theta}(a\sin^2\theta-\lambda). \tag{3}$$

Where,

$$\Sigma = r^2 + a^2\cos^2\theta, R(r) = L^2(r^2+a^2-a\lambda)^2 - \Delta_r(\eta + L^2(\lambda-a)^2), \tag{4}$$

$$\Theta(\theta) = a^2\Delta_\theta L^2 + a^2L^2\cos^2(\theta) - a^2L^2 - 2a\Delta_\theta\lambda L^2 + 2a\lambda L^2 + \Delta_\theta\eta + \Delta_\theta\lambda^2L^2 - \lambda^2L^2\cot \tag{5}$$

KDS

Solutions to these null geodesic equations can be obtained by first introducing the "Mino time"τ parameter or converting the equations to integral forms .

$$\frac{\Sigma}{E}p^{\mu} = \frac{dx^{\mu}}{d\tau} \tag{6}$$

We convert our equations into integral forms as,

$$I_{\theta} = \int_{\theta_s}^{\theta_o} \frac{d\theta}{\pm\sqrt{\Theta(\theta)}}, \tag{7}$$

$$I_r = \int_{r_s}^{r_o} \frac{dr}{\pm\sqrt{R(r)}}, \phi_o - \phi_s = \frac{\left(aL^2\right)\left(a(a-\lambda)+\mathrm{r}^2\right)}{\Delta_r} I_r - L^2 a I_{\phi} + L^2\lambda\bar{I}_{\phi}, \tag{8}$$

$$t_o - t_s = \frac{L^2}{\Delta_r}((r^2+a^2)^2 - a\lambda(a^2+r^2))I_r + a^2L^2I_t - aL^2(a-\lambda)I_{\phi}, \tag{9}$$

Where we have defined,

$$I_{\phi} = \int_{\theta_s}^{\theta_o} \frac{d\theta}{\pm_r\sqrt{\Theta(\theta)}\Delta_{\theta}}, \bar{I}_{\phi} = \int_{\theta_s}^{\theta_o} \frac{d\theta}{\pm_{\theta}\sqrt{\Theta(\theta)}\Delta_{\theta}\sin^2\theta}, I_t = \int_{\theta_s}^{\theta_o} \frac{\cos^2\theta d\theta}{\pm_{\theta}\sqrt{\Theta(\theta)}\Delta_{\theta}}. \tag{10}$$

- The integral forms are related to mino time by $\tau = I_\theta = I_r$.
- By using the mino time parametrization and Jacobi elliptic integrals, we have solved the integrals.

Latitudinal Motion Trajectory

$$\theta_o(\tau) = \arccos\left(-\sqrt{u_+}\nu_\theta sn\left[\left(\tau\sqrt{-u_-\Xi} - \nu_\theta F\left(\varphi_s|k\right)\right) \mid k\right]\right) \tag{11}$$

u_+ and u_- are related to the roots of the angular potential

Azimuthal Motion Trajectory

$$\phi_o - \phi_s = \frac{(aL^2)\left(a(a-\lambda)+\mathrm{r}^2\right)}{\Delta_r}\tau - L^2 aI_\phi + L^2\lambda\bar{I}_\phi \tag{12}$$

Temporal Motion Trajectory

$$t_o - t_s = \frac{L^2}{\Delta_r}((r^2 + a^2)^2 - a\lambda(a^2 + r^2))\tau + a^2 L^2 I_t - aL^2(a - \lambda)I_\phi \tag{13}$$

Where,

$$\Xi = \left(\frac{1}{3}a^2\eta\Lambda + \frac{1}{3}a^2\lambda^2\Lambda L^2 - \frac{2}{3}a^3\lambda\Lambda L^2 + \frac{1}{3}a^4\Lambda L^2 + a^2 L^2\right) \tag{14}$$

$$I_\phi = \frac{1}{\sqrt{-u_-\Xi}}\left[\nu_\theta \Pi(-yu_+, \varphi_s, k) - \nu_\theta \Pi(-yu_+, \varphi_\tau, k)\right], \tag{15}$$

$$\bar{I}_\phi = \frac{1}{\sqrt{-u_-\Xi}}\frac{1}{1+y}\left[\nu_\theta(\Pi(u_+, \varphi_s, k) + y\Pi(-yu_+, \varphi_s, k))\right] - \frac{1}{\sqrt{-u_-\Xi}}\frac{1}{1+y}\left[\nu_\theta(\Pi(u_+, \varphi_\tau \mid k) + y\Pi(-yu_+, \varphi_\tau \mid k))\right], \tag{16}$$

$$I_t = \frac{u_+}{\sqrt{-u_-\Xi}}\left[\nu_\theta J(-yu_+, \varphi_s \mid k) - \nu_\theta J(-yu_+, \varphi_\tau \mid k)\right] \tag{17}$$

$$\Delta_r = \left(1 - \frac{\Lambda r^2}{3}\right)(r^2 + a^2) - 2Mr \tag{18}$$

The parameters $F(x \mid k)$ and $\Pi(n, x \mid k)$ are the Elliptic integrals of first and third kind respectively. Moreover, $J(n, x \mid k)$ is related to the Carlson's integral, R_j, through the relation,

$$J(n, x \mid k) = \frac{1}{3}\sin^3(x) R_J\left(\cos^2(x), 1 - k\sin^2(x), 1, 1 - n\sin^2(x)\right) \tag{19}$$

Examples of selected orbits

Figura 4: Zero Angular Momentum Orbit, $\lambda = 0$. The pink arrow shows the poles. $\theta_1 = 0$, $\theta_4 = \pi$

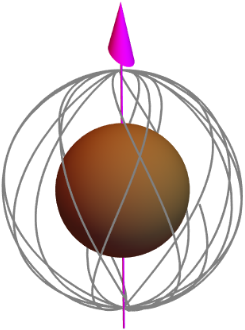

Figura 5: Orbit at $r = 1.76M$, $\theta_1 = 0.737886$ and $\theta_2 = 2.40371$

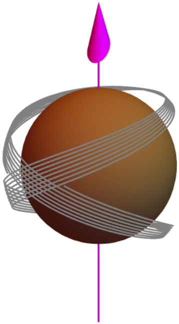

Figura 6: Equatorial circular prograde orbit, $\theta_1 = \pi/2$ and $\theta_2 = \pi/2$

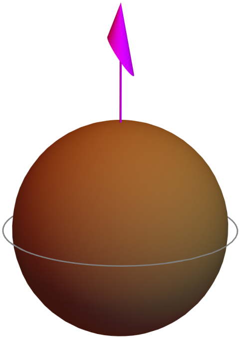

Figura 7: Equatorial circular retrograde orbit, $\theta_1 = \pi/2$ and $\theta_2 = \pi/2$

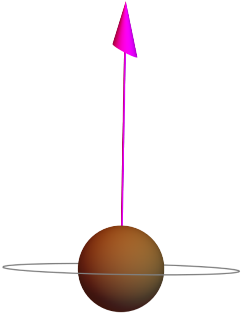

Why do some orbits seem circular and others not circular?

- The motion of these orbits is governed by constants of motion, η and λ: They arise from the symmetries of KdS metric (t, r, θ, ϕ).
- $R(r) = R'(r) = 0$,

$$\eta = -\frac{L^2 r^3 \left(6a^2 \left(\Lambda r^2 (3M + r) - 6M\right) + a^4 \Lambda^2 r^3 + 9r(r - 3M)^2\right)}{a^2 \left(r \left(a^2 \Lambda + 2\Lambda r^2 - 3\right) + 3M\right)^2}, \tag{20}$$

$$\lambda = \frac{r \left(a^2 \left(6 - \Lambda r^2\right) + 3r(r - 3M)\right)}{a \left(r \left(a^2 \Lambda + 2\Lambda r^2 - 3\right) + 3M\right)} + a. \tag{21}$$

Radii at which η vanishes

$$r_{ph+,KdS} = -\frac{2M(y-1)}{(y+1)^2} + 2\sqrt{\frac{M^2((y-14)y+1)}{(y+1)^4}} \cos\left(\frac{\kappa}{3} + \frac{4\pi}{3}\right), \tag{22}$$

$$r_{ph-,KdS} = -\frac{2M(y-1)}{(y+1)^2} + 2\sqrt{\frac{M^2((y-14)y+1)}{(y+1)^4}} \cos\left(\frac{\kappa}{3}\right). \tag{23}$$

The photon region: $[r_{ph+,KdS}, r_{ph-,KdS}]$.

Radius at which λ vanishes.

$$r_{zamo,KdS} = \frac{3M}{a^2\Lambda + 3} + 2\sqrt{\frac{9M^2}{\left(a^2\Lambda+3\right)^2} - \frac{a^2}{3}} \cos\left(\frac{1}{3}\arccos\left[-\frac{9\sqrt{3}M\left(a^2\left(a^2\Lambda+3\right)^2 - 9M^2\right)}{\left(a^2\Lambda+3\right)^3\left(\frac{27M^2}{\left(a^2\Lambda+3\right)^2} - a^2\right)^{3/2}}\right]\right). \quad (24)$$

Is the boundary between co-rorating $[r_{ph+,KdS}, r_{zamo,KdS}]$ and counter-rotating orbits $(r_{zamo,KdS}, r_{ph-,KdS}]$.

How much time do these orbits take to complete half oscillations: Time delay

$$\zeta = \left(\frac{L^2}{\Delta_r}((r^2 + a^2)^2 - a\lambda(a^2 + r^2))\Gamma_\theta + a^2 L^2 \Gamma_t - aL^2(a - \lambda)\Gamma_\phi \right) \tag{25}$$

Figura 8: Time delay around SgrA,with $M = 4 \times 10^6 M_\odot$.

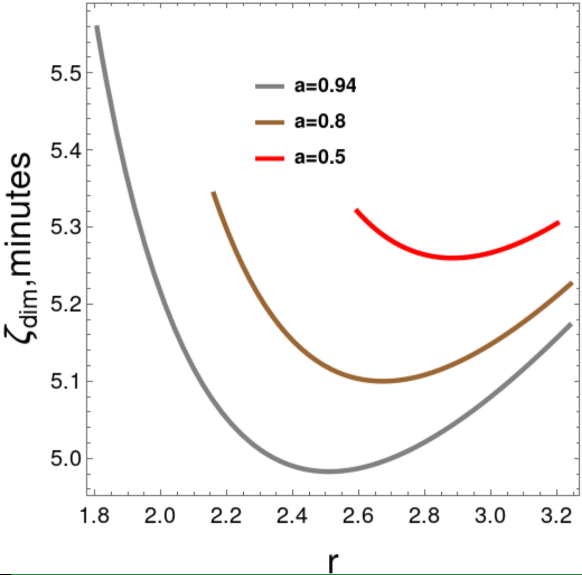

Figura 9: Time delay around M87, with $M = 6 \times 10^9 M_\odot$

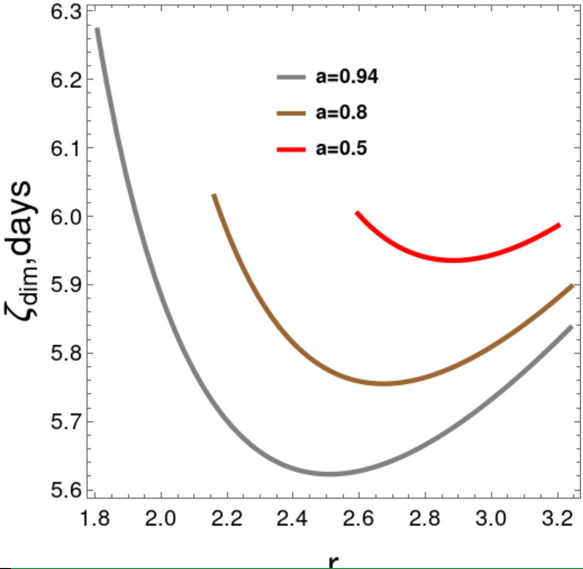

How much azimuthal angle change do these orbits experience in half an oscillation?-**Change in Azimuthal angle**.

$$\delta = \left(\frac{(aL^2)\left(a(a-\lambda)+\mathrm{r}^2\right)}{\Delta_r}\Gamma_\theta - L^2 a\Gamma_\phi + L^2\lambda\bar{\Gamma}_\phi \right) \tag{26}$$

Figura 10: Change in Azimuthal angle parameter.

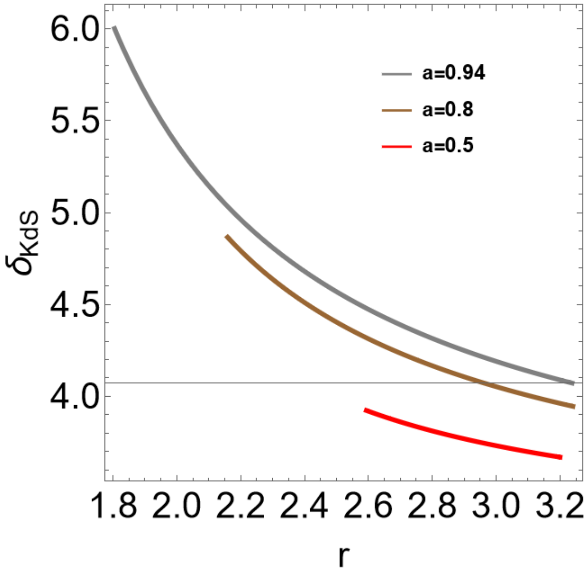

Nearly bound orbits.

Orbits asymptoting bound photon orbits.

Figura 11: The gray orbit is a bound photon orbit at $r_{zamo,KdS} = 2.56M$. The red orbit is a nearly bound photon orbit that experiences a turning point at $r_4 = 2.560052765M$

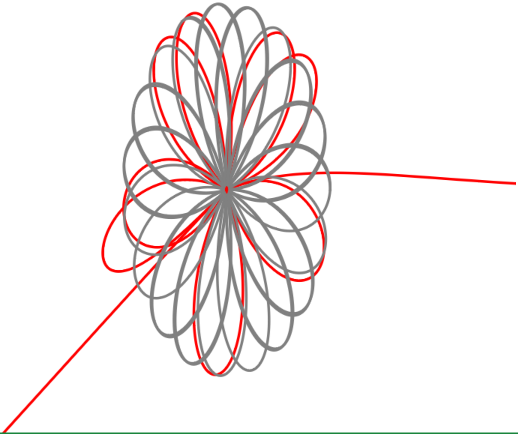

Figura 12: The gray orbit is a bound photon orbit at $r_{zamo,KdS} = 2.56M$. The red orbit is a nearly bound photon orbit that experiences a turning point at $r_4 = 2.749M$

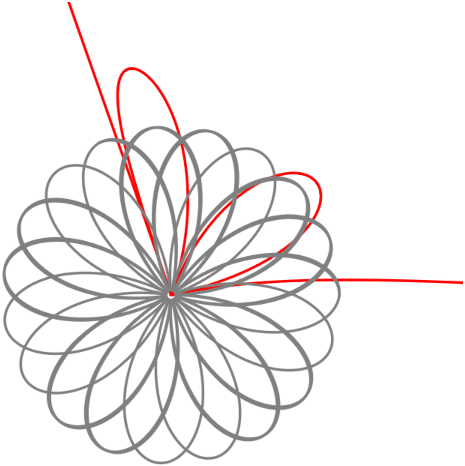

What is the rate of exponential deviation?- **Lyapunov Exponent**

$$\gamma = \sqrt{\frac{1}{3}\Lambda\left(a^2 + 6r^2\right)\left(L^2(a-\lambda)^2 + \eta\right) + L^2\left(a^2 - \lambda^2 + 6r^2\right) - \eta\Gamma_\theta}. \tag{27}$$

Besides giving the rate of exponential deviation, this parameter also controls the demagnification of the subrings.

Figura 13: Lyapunov exponent for observers inclined at 30°.

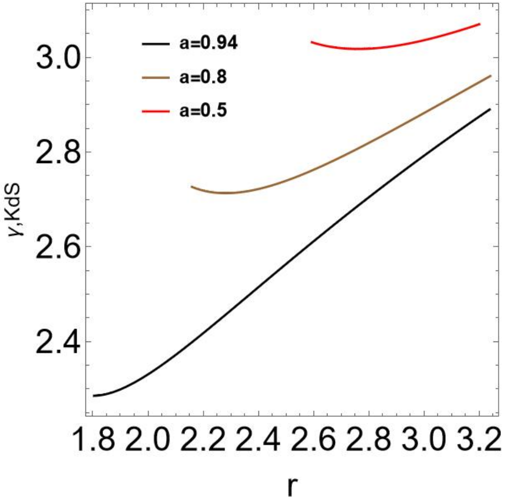

Figura 14: Lyapunov exponent for observers inclined at 90°.

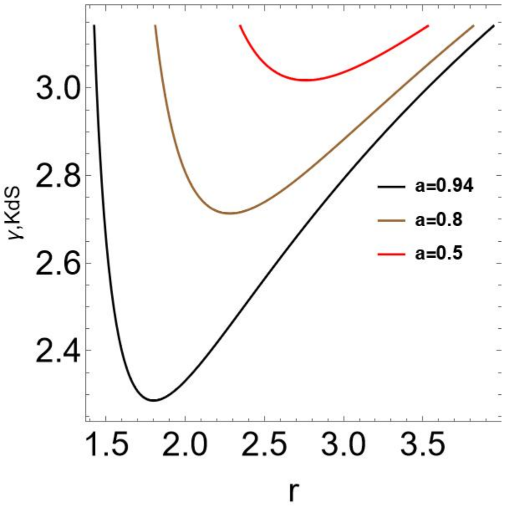

Relationship of the critical parameters to Quasinormal Modes.

- QNMs: $\omega = \omega_{\mathcal{R}} - i\omega_I$.
- These frequencies are indexed by the overtone number n, azimuthal number m and multipole l.
- In the high frequency limit, $l >> 1$, there exists a geometric correspondence between quasinormal modes and bound photon orbits, $\omega_{\mathcal{R}}$:Orbital frequency, ω_I:time-Lyapunov Exponent $\gamma_t = \gamma/\zeta$,

$$\gamma_{t,KdS} = \frac{\Gamma_\theta \sqrt{\frac{1}{3}\Lambda\left(a^2+6r^2\right)\left(L^2(a-\lambda)^2+\eta\right)+L^2\left(a^2-\lambda^2+6r^2\right)-\eta}}{\frac{L^2\Gamma_\theta\left(\left(a^2+r^2\right)^2-a\lambda\left(a^2+r^2\right)\right)}{\Delta_r}+a^2L^2\Gamma_t-aL^2(a-\lambda)\Gamma_\phi} \tag{28}$$

- Evaluating this relation numerically correctly yields the same results as the time-Lyapunov exponent that has been obtained in KdS in the eikonal limit.

Analytical Ray Tracing

Finite distance observers

Figura 15: Observers at an arbitrary distance from the black hole.

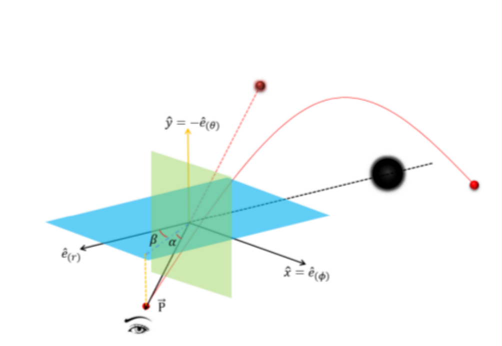

Constants of Motion

$$\lambda = \frac{-\Delta_\theta \left(a^2 + r_o^2\right)\left(x\left(a^2 + r_o^2\right) + ar_o\right) + a^2 \Delta x \sin^2\left(\theta_o\right) + a\Delta r_o}{-a\Delta_\theta \left(x\left(a^2 + r_o^2\right) + ar_o\right) + a\Delta x + \Delta r_o \csc^2\left(\theta_o\right)}, \quad (29)$$

$$\eta = \frac{L^2 r_o^2 \left(-a^2\left(\Delta_\theta - 1\right) + 2a\lambda\left(\Delta_\theta - 1\right) - \lambda^2 \Delta_\theta\right)}{\Delta_\theta r_o^2} + \frac{L^2 r_o^2\left(\lambda^2 \csc^2\left(\theta_o\right) - a^2\cos^2\left(\theta_o\right)\right) + \left(p^t\right)^2 y^2}{\Delta_\theta r_o^2} \quad (30)$$

Escaping Orbits

$$R(r) = L^2(r^2 + a^2 - a\lambda)^2 - \Delta_r(\eta + L^2(\lambda - a)^2), \tag{31}$$

$$r_o^E[G_\theta] = \frac{r_3(r_1 - r_4)\mathrm{sn}^2\left(\frac{G_\theta}{g_E} + \nu_r F(\varphi_{E,s}|k_E)\middle| k_E\right) + r_4(r_3 - r_1)}{(r_1 - r_4)\mathrm{sn}^2\left(\frac{G_\theta}{g_E} + \nu_r F(\varphi_{E,s}|k_E)\middle| k_E\right) - r_1 + r_3}. \tag{32}$$

$$G_\theta = \frac{1}{\sqrt{-u_- \Xi}}\left[2mK(k_E) + (-1)^m Sign((p^\theta)_o)F(\psi_s, k_E) - Sign((p^\theta)_o)F(x_o, k_E)\right]. \tag{33}$$

$$k_E = \frac{(r_4 - r_1)(r_3 - r_2)}{(r_4 - r_2)(r_3 - r_1)}. \tag{34}$$

Figura 16: Direct images for $\theta_o = 80^\circ$

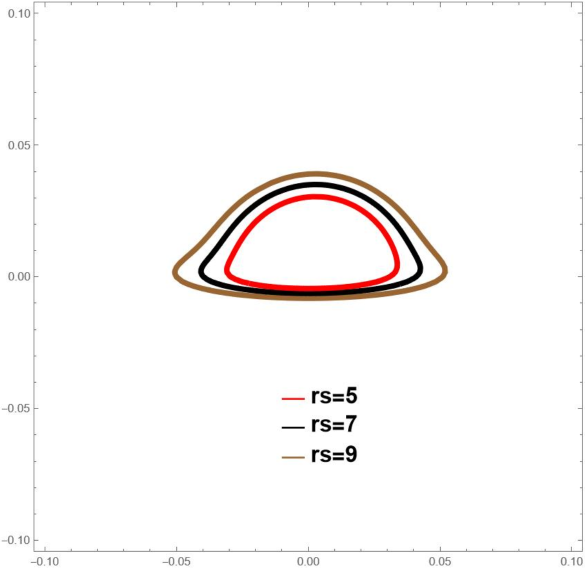

Figura 17: Direct images for $\theta_o = 50^\circ$

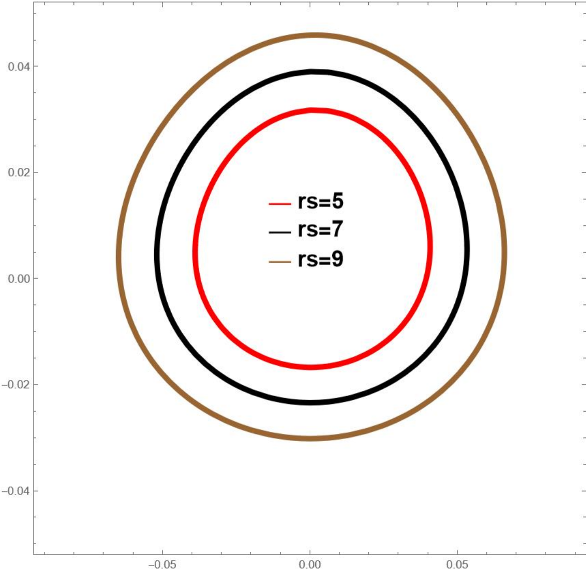

Figura 18: Direct images for $\theta_o = 10^\circ$

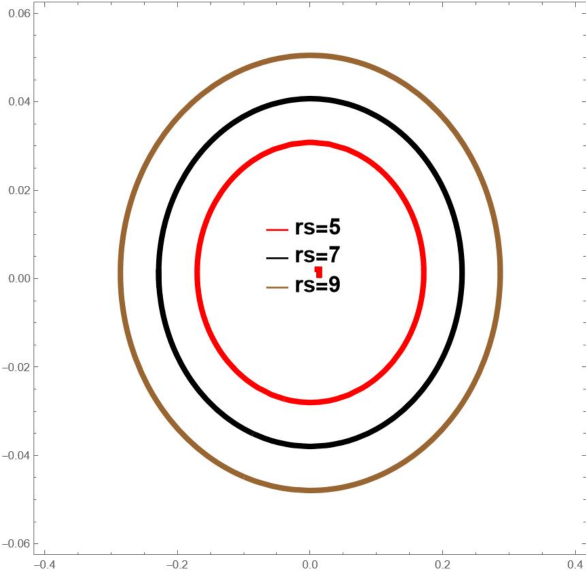

Figura 19: Direct images for $\theta_o = 80^\circ$ for different r_o.

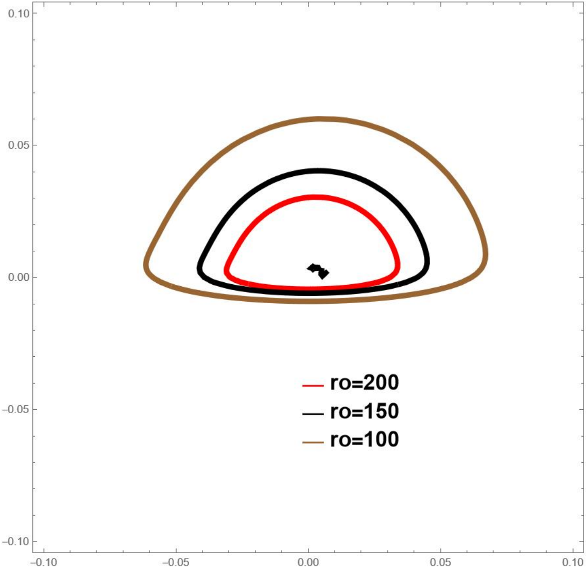

However, the equation breaks down for higher order images!

Thus performing the analytical ray tracing for lensed images requires approximation of the radial integrals.

Conclusion

- We have analyzed bound photon orbits in KdS space time.
- The solutions have been obtained in terms of Jacobi elliptic integrals.
- We have also analyzed the critical parameters controlling the structure of the photon ring.
- Nearly bound photon orbits have been obtained.
- Considering observers at an arbitrary distance from the black hole, we have obtained the direct images for equatorial disks.
- Ongoing: Obtaining lensed images for equatorial disks.


OBRIGADA